Investigating stem cells in human colon by using methylation patterns

Yasushi Yatabe*†, Simon Tavaré‡, and Darryl Shibata*§

*Department of Pathology, University of Southern California School of Medicine, Los Angeles, CA 90033; and ‡Departments of Biological Sciences, Mathematics, and Preventive Medicine, University of Southern California, Los Angeles, CA 90089

Edited by Bert Vogelstein, Johns Hopkins Oncology Center, Baltimore, MD, and approved July 12, 2001 (received for review May 7, 2001)

The stem cells that maintain human colon crypts are poorly characterized. To better determine stem cell numbers and how they divide, epigenetic patterns were used as cell fate markers. Methylation exhibits somatic inheritance and random changes that potentially record lifelong stem cell division histories as binary strings or tags in adjacent CpG sites. Methylation tag contents of individual crypts were sampled with bisulfite sequencing at three presumably neutral loci. Methylation increased with aging but varied between crypts and was mosaic within single crypts. Some crypts appeared to be quasi-clonal as they contained more unique tags than expected if crypts were maintained by single immortal stem cells. The complex epigenetic patterns were more consistent with a crypt niche model wherein multiple stem cells were present and replaced through periodic symmetric divisions. Methylation tags provide evidence that normal human crypts are long-lived, accumulate random methylation errors, and contain multiple stem cells that go through ''bottlenecks'' during life.

Most of the information on intestinal stem cells has been inferred in mice by using histologic markers. For example, crypts at chimeric patch boundaries are initially polyclonal but subsequently display only a single marker by 2 weeks after birth (1). This process implies that crypts are monoclonal because they are derived from single progenitors. Mutagenesis can also induce crypt heterogeneity that subsequently declines as markers become uniformly present or absent. These observations suggest that crypts are maintained by small numbers (between 1–40) of variously defined stem cells (2, 3). This stem cell architecture may protect against neoplasia as most non-stem cells differentiate and die within a week (4).

Less is known about human crypts. Human and murine dynamics may be similar as some patients demonstrate mutant crypt frequencies consistent with those measured in the mouse (5). Human studies are difficult because strategies that directly mark cell fates, such as aggregation chimeras and mutagenesis, are impractical in human beings. Longer lifetimes and larger human crypts may pose unique challenges for crypt maintenance and prevention of neoplasia.

Alternatives to experimentally created visible markers are endogenous sequences that become polymorphic with aging. Related cells should share such sequence polymorphisms. Although low mutation frequencies hinder this strategy, recent studies demonstrate changes in methylation of some CpG islands with aging in normal human colon (6, 7). Methylation exhibits somatic inheritance and random site autonomous changes (8, 9) that accumulate more frequently than mutations (10). Methylation can modulate transcription and chromatin structure (11, 12), but some changes may reflect random errors, especially at CpG sites of unexpressed genes. Such age-related errors can potentially encode binary (methylated vs. unmethylated) information strings in adjacent CpG sites, creating tags that can be read with bisulfite sequencing. Although human colon crypts presumably originate from single progenitors (1–3), they could become quasi-clonal (contain multiple tags) depending on epigenetic and stem cell dynamics. As an alternative to histologic examination, it may be possible to recreate crypt histories by comparing epigenetic tags within and between crypts.

Methods

Isolation of Single Crypts. Individual crypts (>95% epithelial cells) were isolated (13) from ≈1–2 cm^2 normal patches of 10 fresh colectomy specimens (Table 1). DNA was extracted in a 10-μl solution (100 mM Tris·HCl/4 mM EDTA, pH 8.0/200 μg/ml of proteinase K) for 4 hours at 56°C, followed by boiling for 5 min. Cytosine bases were converted by bisulfite treatment (14), using an agarose bead method (15). Agarose bead sizes were 20–30 μl. DNA was also extracted from microdissected epithelial regions of four paraffin-embedded colons to estimate methylation of younger individuals.

Methylation Analysis. Patterns were analyzed for three loci (Fig. 1): CpG islands in myogenic factor 3 (MYOD1; GenBank accession no. AF027148; nucleotides 9,432–9,557), cardiac-specific homeobox (CSX; GenBank accession no. NM004387; nucleotides 1,271–1,377), and an X-chromosome CpG-rich region in biglycan (BGN; GenBank accession no. M65151; nucleotides 519–648). Age-related methylation has been demonstrated for MYOD1 (6) and CSX [Mint 23 (7)]. BGN is a small cellular or pericellular matrix proteoglycan primarily expressed in connective tissue (16). The serial analysis of gene expression database (www.ncbi.nlm.nih.gov/SAGE) failed to yield tags specific for these loci in normal or neoplastic colon tissues.

An average of 7.5 crypts (range 7–9) per patient were examined for each locus. Primers amplified only bisulfite-converted DNA and were (5′-3′) MYOD1: F-GGAGGGGATTTTTAATTTGGGT and R-AAACCCAATCCTTCTTCCCTAA; CSX: F-GGAGATTTAGGAATTTTTTTTGTTTT and R-ACACCAAACTACAAAATCACTCATTA; and BGN: F1-TTTAGGAGTGAGTAGTTGTTTTTGGTT, F2-TAGGAGTGAGTAGTTGTTTTCGGTT, and R-ACCAACCCTACCTAAAAAAAAAAAA.

Two forward BGN primers were used to avoid bias caused by an internal CpG site. Approximately half the bead was amplified with 42 PCR cycles (60°C annealing temperature) in 4 independent reactions by using AmpliTaq Gold polymerase (Perkin–Elmer), 4 mM $MgCl_2$, and 1 μM of each primer in 50-μl volumes. PCR products were combined, and the mixtures were cloned (Topo-TA cloning kit, Invitrogen). At least 5 clones or molecules per locus (averages of 7.5 for MYOD1, 7.8 for CSX, and 7.2 for BGN) per crypt were sequenced. Sequences with incomplete

This paper was submitted directly (Track II) to the PNAS office.

Abbreviations: MYOD1, myogenic factor 3; CSX, cardiac-specific homeobox; BGN, biglycan.

See commentary on page 10519.

†Present address: Department of Pathology and Molecular Diagnostics, Aichi Cancer Center, Nagoya 464-8681, Japan.

§To whom reprint requests should be addressed at: University of Southern California School of Medicine, 1200 North State Street, Box 736, Los Angeles, CA 90033. E-mail: dshibata@hsc.usc.edu.

The publication costs of this article were defrayed in part by page charge payment. This article must therefore be hereby marked "*advertisement*" in accordance with 18 U.S.C. §1734 solely to indicate this fact.

Table 1. Patients and loci

Patient	Age/Sex	Site	Disease	Loci examined
A	88 F	Proximal	Cancer	MYOD CSX
B	37 M	Distal	IBD†	MYOD CSX
C	75 F	Distal	Prolapse	MYOD CSX
D	41 M	Unknown	IBD	MYOD CSX BGN
E	65 F	Distal	Cancer	MYOD CSX
F	63 M	Unknown	Cancer	MYOD CSX BGN
G	67 F	Unknown	IBD	MYOD CSX
H	76 M	Distal	Cancer	MYOD CSX BGN
I	40 M	Distal	Carcinoid	MYOD CSX BGN
M	87 M	Distal	Cancer	BGN
Child A*	1 M	Proximal	Colitis	MYOD CSX BGN
Child B*	15 M	Distal	Trauma	MYOD CSX BGN
Child C*	18 M	Distal	Trauma	MYOD CSX BGN
Child D*	0.2 M	Distal	Obstruction	MYOD CSX BGN

*DNA was extracted from microdissected fixed colon.
†IBD, inflammatory bowel disease (patients B and D had ulcerative colitis and patient G had Crohn's disease; uninvolved areas were examined).

bisulfite conversion (Cs at non-CpG sites) were rare (<2% of all molecules) and excluded from analysis. Mutations at non-CpG sites were rare (<0.0005 per nucleotide).

To examine whether sampling could detect crypt diversity, seven crypts were combined and then subdivided into seven "mixed" crypt extracts. Six mixed crypts from three patients were analyzed at CSX and MYOD1 as described previously. Diversity (see below) of the mixed crypts should be greater than single crypts and equivalent to the diversity calculated from the molecules of all individual crypts. Distances of the mixed crypts were on average 1.4 times greater than the average single crypt, and 89% of the average distances of all molecules from the individual patients, which was consistent with an ability to detect heterogeneous crypts with our sampling scheme.

Calculations. A number of statistics that describe methylation patterns were used. Percent methylation is determined by averaging sites from all molecules from each crypt. The number of unique tags is the number of different tags found in each crypt. Average percent crypt methylation and unique tag number are the means of crypt values. Diversity (or epigenetic distance between molecules) between a pair of tags is calculated as the number of differences at each CpG site. For example, if a methylated site is coded as a 1 and an unmethylated site is coded as a 0, the distance between 01001 and 00101 is 2. Maximum distances between two molecules are 5, 8, and 9 for MYOD1, CSX, and BGN, respectively. Intracrypt distance is the average difference of all possible pairs of molecules within a crypt. Average intracrypt distance is the mean of all intracrypt distances. Intercrypt distance is the average difference of all possible pairs of molecules chosen from different crypts. A polymorphism eliminated one BGN CpG site for patient M and calculations were based on eight sites.

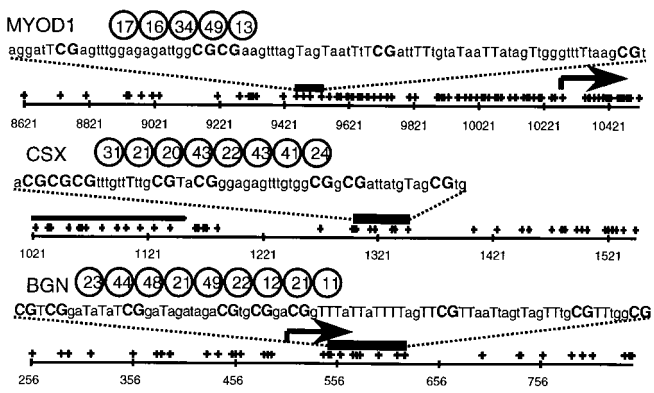

Fig. 1. Methylation tags. CpG sites are indicated by + marks and transcription start sites are indicated by arrows. The tags are in different locations: MYOD1 5′ to the promoter, CSX in the 3′ untranslated region, and BGN 3′ to the promoter. Cumulative percent methylation from all patients and tags are indicated by numbers within circles representing the 5, 8, and 9 CpG sites of the three tags. Bisulfite-treated sequences are illustrated with converted Cs indicated by capital Ts and CpG sites in bold.

Results

Drift can record relationships between cells. More closely related cells share alterations whereas less closely related cells have greater differences. Sequence differences within crypts reflect numbers of stem cells and how they divide (Fig. 2). Crypts may be maintained by small numbers of immortal stem cells or by niches where stem cells undergo random loss with replacement. Differences between these scenarios may be small because each cell within a stem cell niche may replace itself like an immortal stem cell >90% of the time. However, random stem cell loss with replacement eventually leads to sequential "bottlenecks" where all "stem" cells within the niche are related to a new most recent common ancestor. Bottlenecks never occur with immortal stem cells. Therefore, over decades, crypts maintained by multiple immortal stem cells will contain increasingly diverse sequences with numbers of unique sequences proportional to numbers of stem cells. For a niche, crypt sequences will be more closely related, and numbers of unique sequences within each crypt will be variable and depend on the time since a last common crypt ancestor.

To apply this molecular bookkeeping strategy to epigenetic patterns requires evidence of drift. Crypts similar at birth [initially unmethylated (6, 7)] should become different over decades. Unlike histologic markers limited to two states (present or absent), multiple methylation tags are possible. When there are N CpG sites, there are 2^N possible tags, or 32, 256, and 512 possible unique tags for MYOD1, CSX, and BGN. Methylation at the three examined loci (Fig. 1) is unlikely to be under selection because the loci are not significantly expressed in normal or neoplastic colon. Single crypts were sampled from 10 patients, and tags were read by sequencing cloned PCR products after bisulfite treatment (Table 1). Multiple unique tags were present in some crypts, and tags were often different between crypts, which is consistent with random tag drift (Fig. 3). For example, none of the methylated BGN tags were the same between crypts in patient F.

Although tags were different within crypts, the tags were related. Fluctuations with sample sizes were plotted (Fig. 4). Percent methylation and epigenetic distances were relatively stable after five molecules were examined from a crypt. Small numbers of tags may accurately sample these values when crypt cells are related. Small numbers of molecules did not fully sample crypt diversity because new tags could be found even after 16 molecules. Many unique crypt tags suggest multiple stem cells, which is not unexpected because murine crypts may contain as many as 40 stem cells (3).

Quasi-Clonal Human Crypts. Methylation revealed differences between morphologically identical crypts. Average numbers of unique tags per crypt were similar between individuals (2.6 for MYOD1, 3.1 for CSX, and 2.4 for male patients at the X-chromosome locus BGN). More consistent with a niche scenario, numbers of unique tags per crypt were variable (Fig. 5*A*). Maximum observed numbers of unique tags were 8, 9, and 7 (of 11, 18, and 8 sampled molecules), respectively, per crypt. These numbers exceed the one or two tags expected for a strictly

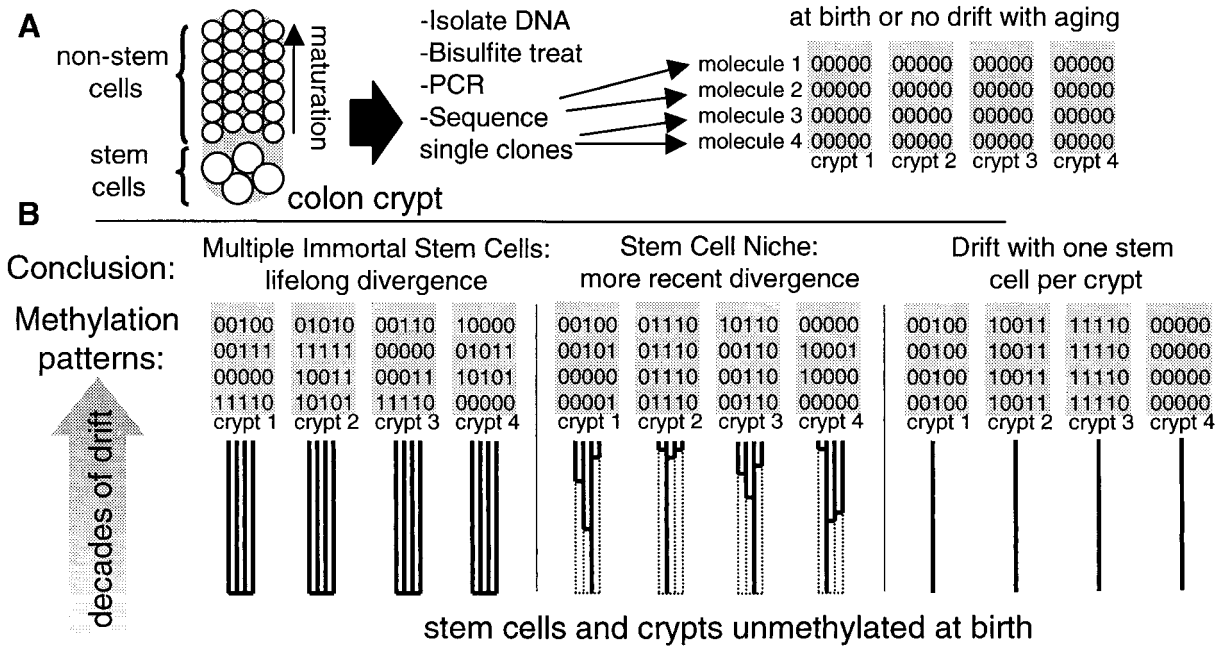

Fig. 2. (*A*) Methylation tags represented as binary strings (0 = unmethylated and 1 = methylated) are sampled from individual crypts. Crypts contain unmethylated tags at birth and if tags do not drift. (*B*) When tags drift, they may differ within and between adult crypts. Differences depend on stem cell numbers and whether they are immortal or can be lost with replacement (stem cell niche). Trees illustrate these different scenarios. If stem cells are immortal, tags will reflect lifelong divergence, and numbers of unique tags will be proportional to numbers of crypt stem cells. In contrast, stochastic bottlenecks recur with a stem cell niche, and some unique tags will be lost. Numbers of unique tags and differences between tags within a crypt will be variable and reflect the time since the last bottleneck. Quantitative comparisons of methylation tags between and within crypts can distinguish between these scenarios.

monoclonal population. Most normal human crypts are quasiclonal with respect to methylation.

Epigenetic variation could be generated with multiple long-lived stem cells or in non-stem cells during crypt epithelial maturation. To determine whether new tags are frequently created during the ≈1 week required for maturation (2, 3, 17), patterns were compared between seven bisected crypt regions. Consistent with stem cell origins for most methylation patterns, upper and lower crypt portions contained similar tags, although frequencies were sometimes different (Fig. 3). Simulations were also consistent with relatively few methylation changes during epithelial maturation because the estimated methylation error rate was 2×10^{-5} per division (see below).

Mosaic Methylation Increases with Aging. Average crypt methylation increased with aging (Fig. 5*B*). This age-related process was complex because methylation varied between crypts within individuals. Crypts with greater than 40% methylation were present in younger individuals (<50 years old), and crypts with less than 5% methylation were present in older individuals (>60 years old). Normal human colon becomes a methylation mosaic.

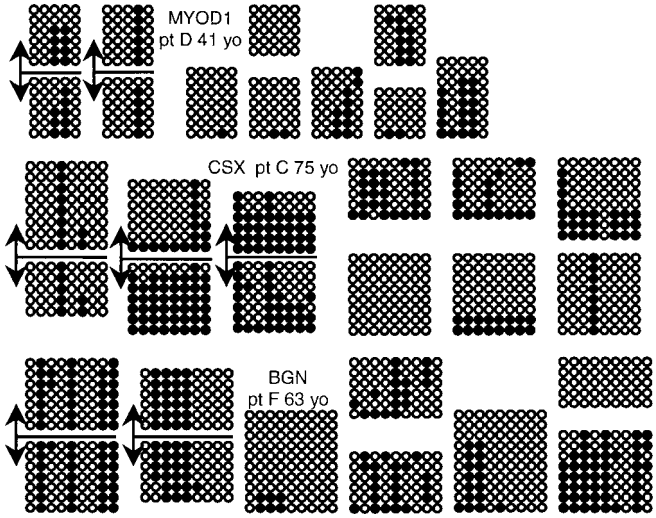

Fig. 3. Mosaic crypts. Each horizontal line represents one tag and each group represents tags from one crypt. Methylated sites are filled circles. Arrows separate tags from upper and lower bisected crypt regions.

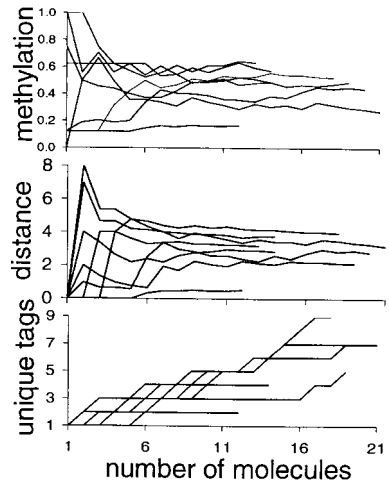

Fig. 4. Fluctuations in crypt values with sampling. Methylation and distances within crypts are relatively stable after five tags are sampled. In contrast, unique tags are still found as more molecules are sampled.

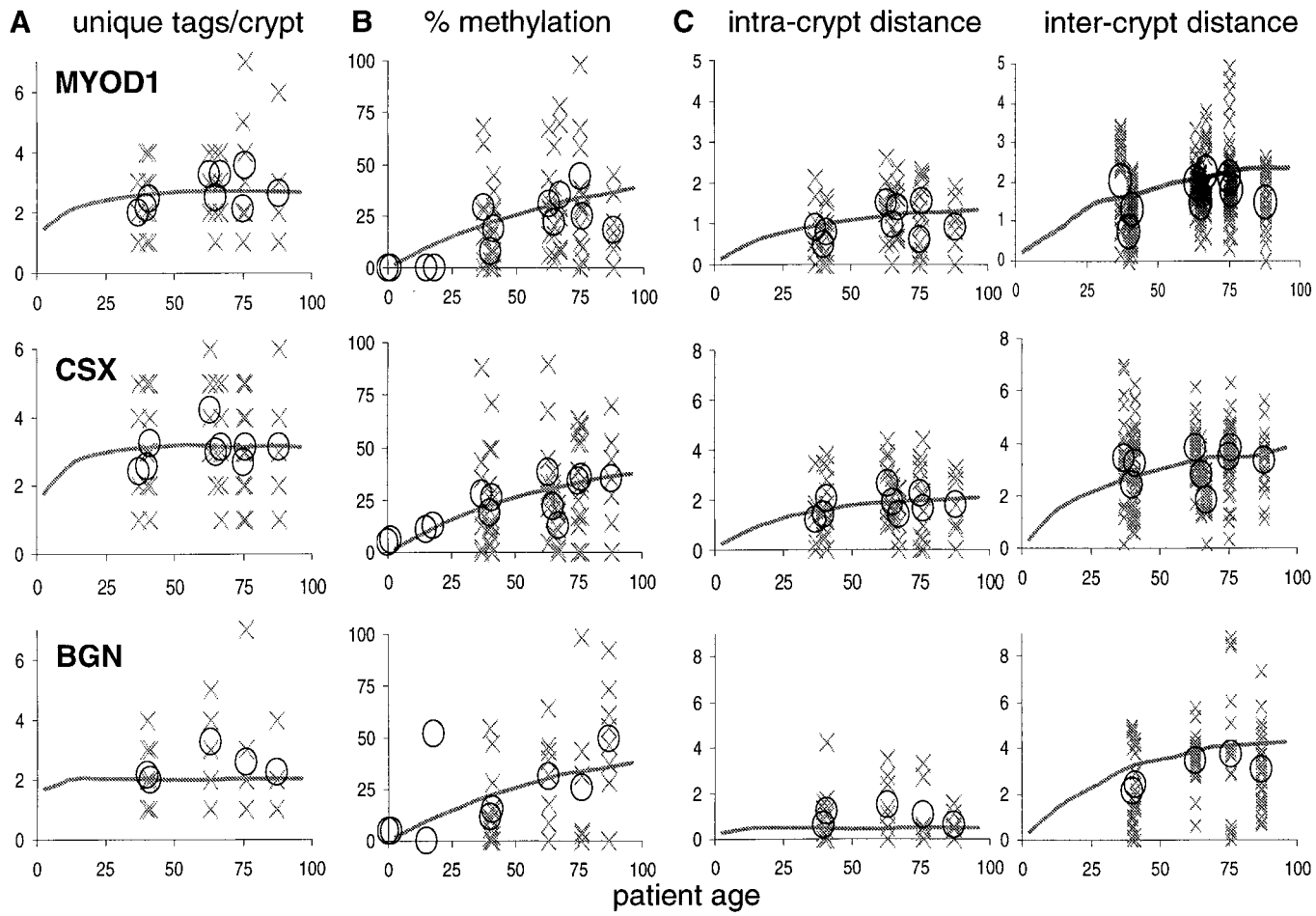

Fig. 5. Tag variability between and within individual crypts. (*A*) Numbers of unique tags were variable between crypts although average numbers of unique tags were relatively stable with aging. (*B*) Methylation increases with aging. (*C*) Intracrypt distances were smaller compared with intercrypt distances. Individual crypt values (''X'') and patient averages (''O'') are illustrated. Simulated average values (solid lines) with 64 stem cells and 95% asymmetric divisions are superimposed on the experimental data (see Fig. 7).

Methylation frequencies were unequal between CpG sites (Fig. 1). These differences may be the result of stochastic variation and a tendency for some sites to become methylated. Overall, methylation resembled a random process (8, 9). There was also variability between tags and CpG islands within a crypt. Hyper- and hypomethylated CSX or MYOD1 tags were present in some crypts (Fig. 3). Percent methylation between MYOD1 and CSX did not correlate within single crypts (Fig. 6). Methylation of one allele does not predict the status of the other allele or another CpG island.

Aging of Colon but Not Crypts. Methylation patterns differed between crypts but were more similar within crypts (Fig. 3). Distances between crypts and within crypts were variable, with greater intercrypt compared with intracrypt distances (Fig. 5*C*). Diversity of the colon is greater than individual crypts.

Crypt Dynamics. To understand further the experimental observations, crypts were simulated starting with unmethylated tags, a methylation error rate of 2×10^{-5} per CpG site per division, and one division per day. In our model, a crypt always has N stem cells, as well as a number of non-stem cells. Each stem cell produces two cells, of which either 0, 1, or 2 are stem cells with probabilities q, p, and q, respectively (where $p + 2q = 1$), constrained to ensure a total of N stem cells in the next generation (18). Non-stem cells always produce non-stem cell offspring (see supporting information, which is published on the PNAS web site, www.pnas.org). There are two models we wish to contrast. The first, which has $p = 1$, corresponds to immortal

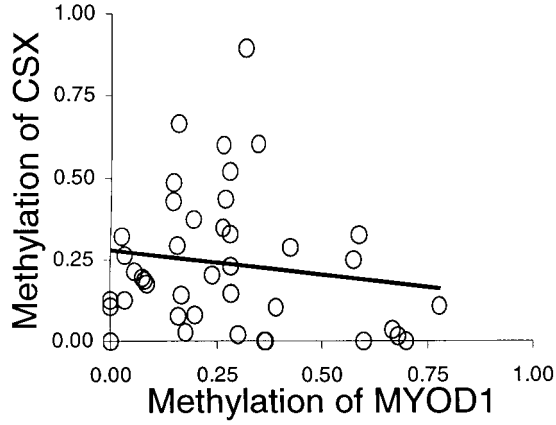

Fig. 6. Lack of correlation between average methylation of CSX and MYOD1 within single crypts. Correlation coefficient is −0.17.

Table 2. Observed and expected variance of unique tags per crypt

Stem cell model		2 immortal, $p = 1.0$	64-cell niche, $p = 0.95$	256-cell niche, $p = 0.89$
Observed variance		Variance under model, average (CI)		
			CSX	
A	2.5	0.37 (0.14–0.90)	0.83 (0.24–2.1)	1.1 (0.24–2.7)
B	2.3	0.47 (0.14–1.1)	0.84 (0.24–2.3)	1.0 (0.24–2.3)
C	1.8	0.35 (0.11–0.78)	1.0 (0.28–2.3)	1.3 (0.36–2.9)
D	1.9	0.50 (0.12–1.1)	0.86 (0.21–2.1)	1.1 (0.27–2.8)
E	2.0	0.44 (0.14–0.90)	0.83 (0.14–2.2)	1.1 (0.24–2.8)
F	0.94	0.39 (0.19–0.78)	0.94 (0.25–2.2)	1.2 (0.28–2.4)
G	2.5	0.42 (0.14–1.0)	0.83 (0.14–2.1)	0.98 (0.24–2.3)
H	1.8	0.45 (0.14–1.0)	0.81 (0.24–2.2)	1.0 (0.24–2.5)
I	1.3	0.46 (0.14–1.0)	0.99 (0.24–2.2)	1.2 (0.29–3.0)
			BGN	
D	0.67	0.073 (0–0.33)	0.63 (0.24–1.5)	0.79 (0.24–1.9)
F	2.3	0.035 (0–0.21)	0.80 (0.21–2.3)	1.0 (0.27–2.6)
H	4.3	0.029 (0–0.14)	0.75 (0.14–1.9)	0.90 (0.14–2.2)
I	1.1	0.052 (0–0.24)	0.68 (0.14–1.7)	0.84 (0.14–2.0)
M	1.4	0.031 (0–0.21)	0.67 (0.21–1.6)	0.90 (0.21–2.0)

Variance is based on the distribution of unique tags per crypt per patient. Predicted variances are based on simulations specific for the numbers of crypts and tags experimentally sampled from each patient. Confidence intervals (CI) reflect upper and lower 2.5% of simulated values.

stem cells. The second, for which $0 \leq p < 1$, corresponds to a stem cell niche architecture (19).

The immortal model with $N = 2$ fits average crypt values satisfactorily, whereas the stem cell niche model fits well with N of at least 4 (Fig. 8, which is published as supporting information on the PNAS web site). However, the two models predict very different behaviors for the variance of the average crypt values. Variances in numbers of unique tags per crypt within individuals were always greater than the simulated 97.5th percentile for immortal stem cells, but most were between the simulated 2.5th and 97.5th percentiles for crypt niche models (Table 2). The size of this niche could not be determined because from 4 to 512 cell niches with $p = 0.98$ to $p = 0.75$, respectively, were consistent with the data (Fig. 9, which is published as supporting information on the PNAS web site). Identical crypt niche and epigenetic parameters applied to all three loci examined, largely recapitulating both average values and scatter of individual crypts (Figs. 5 and 9).

A crypt at different times may have distantly or closely related cells because of random stem cell loss and replacement. For a 64-stem cell niche [assuming the 95% asymmetrical division estimated for murine crypts (20); Fig. 7], the most recent common ancestral stem cell of the stem cells present at a given time is on average ≈3,000 divisions ago (with a 95% interquantile range of 1,000–7,000). A bottleneck recurs on average every 8.2 years. If 1 of 64 crypt stem cells was mutated, the mean time for this mutant stem cell to become completely dominant or extinct in our model was 220 days (with a 95% interquantile range of 2–1,900 days), which is consistent with 1-year clonal stabilization times inferred from human crypt heterogeneity after irradiation (5).

Discussion

Murine crypt architecture is inferred from intervals in which visibly mixed crypts become homogeneous (1–3). This approach can also be applied to humans by comparing epigenetic tags within and between morphologically identical crypts. Methylation tags allow fate-mapping because their patterns are somatically inherited (10) but drift within a lifetime to become polymorphic. Heterogeneous methylation patterns have been observed in other adult human tissues (21), tumors (9, 22), and within aberrant colon crypts (23). Changes in human tags with aging can potentially yield fate maps for a variety of adult tissues, extending observations decades beyond those possible in mice.

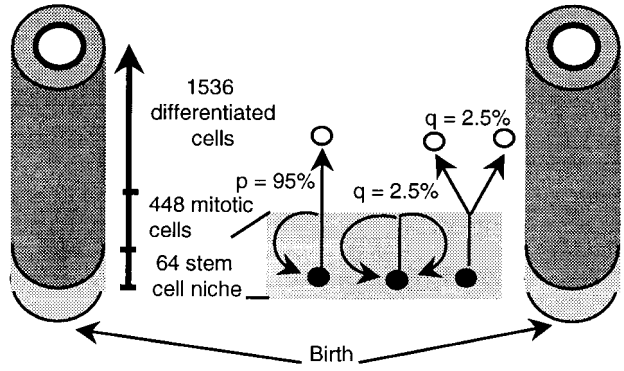

Fig. 7. Simulations modeled 2,048 cell crypts with varying numbers of stem cells, modes of stem cell division (asymmetric or symmetric), methylation error rates, and numbers of divisions (0–35,000). Methylation was site-autonomous and the same for all divisions (including non-stem cell divisions) with an error rate (either methylation or demethylation) of 2×10^{-5} per CpG site per division. The experimental process of sampling eight molecules from a crypt was also simulated. A 64-stem cell niche with 95% asymmetric divisions is illustrated.

Methylation patterns were extremely variable or mosaic between crypts within an individual. Percent methylation did not correlate between CpG islands within single crypts. Simulations suggest methylation with aging (6) is a consequence of stochastic errors that begin from birth rather than loss of an ability to maintain unmethylated CpG sites. The estimated error rate of 2×10^{-5} per CpG site per division in human crypts is lower than observed in tissue culture (8, 24). However, culture may effect methylation patterns, and some measurements occurred after experimental demethylation. This estimated epigenetic error rate is about 4 orders of magnitude higher than human DNA replication [10^{-9} per base (25)]. Drift would inherently increase average methylation with aging because the loci, like most CpG islands (26), were initially unmethylated. Fidelity may differ at other CpG sites because of selection or different mechanisms of methylation.

Despite clonal origins and small sizes (≈2,000 cells), many normal human colon crypts contained multiple unique tags and were quasi-clonal. Multiple crypt tags likely reflect multiple long-lived stem cells. Stem cell definitions are variable but all include self-renewal through asymmetric divisions. The current simulations define stem cells through self-renewal and infer "stemness" as a property of a compartment or niche (19) rather than an intrinsic cell-determined fate. Variability of unique tag numbers between crypts is greater than predicted for immortal stem cells and more consistent with the stochastic properties of a stem cell niche. This crypt niche is functionally similar to the germ cell niche recently characterized in *Drosophila* (27–29). The exact number of cells in this niche is uncertain and may vary between crypts and individuals. Similar to mice (3), as many as 10% of human crypt cells may exhibit stem cell-like properties.

Symmetric divisions allow stem cell removal or expansion that effectively oscillates and limits intracrypt diversity. Somatic losses of stem cells inferred after mutagenesis appear to occur in unperturbed normal human crypts. Bottlenecks or reduction to a new single most recent common crypt progenitor are predicted to recur several times during life, superficially resembling the

clonal succession of tumor progression (30). Stem cell multiplicity may help ensure crypt integrity and survival, leading to mosaic methylation between crypts.

Other models could account for mosaic methylation, and many assumptions cannot be directly tested and may differ between crypts or individuals. However, it is currently impossible to isolate or identify crypt stem cells, and methylation tags allow noninvasive systematic studies of normal human crypts. Crypt histories seem to be at least partially recorded in tags as a simple model consistent with murine studies that was able to organize complex methylation patterns from different patients.

Methylation tags provide evidence that normal human crypts are long-lived, contain multiple stem cells, undergo continuous bottlenecks, and accumulate random methylation errors at some loci. Tags reveal two ongoing counteracting but otherwise invisible forces shaping crypt diversity—drift and extinction. Drift is difficult to document because mutations are rare in normal human tissues (31). Labile epigenetic markers readily reveal differences within and between otherwise morphologically identical crypts. A stem cell niche architecture minimizes the risk of cancer (4), and periodic stem cell losses would eliminate some alterations that occur with aging. These dynamics may be important from a perspective of early multistep tumorigenesis because global hypomethylation (32) or mutagenesis before crypts become monoclonal (33) and respectively decrease or increase adenomas in Min mice. Methylation tags or other sufficiently labile molecular clocks (34) provide opportunities to investigate otherwise invisible cell fates during human somatic evolution.

This work was supported by National Institutes of Health Grant CA70858 (to D.S.) and by National Science Foundation Grant BIR95-04393 (to S.T.).

1. Schmidt, G. H., Winton, D. J. & Ponder B. A. J. (1988) *Development (Cambridge, U.K.)* **103,** 785–790.
2. Potten, C. S. & Loeffler, M. (1990) *Development (Cambridge, U.K.)* **110,** 1001–1020.
3. Bach, S. P., Renehan, A. G. & Potten, C. S. (2000) *Carcinogenesis* **21,** 469–476.
4. Cairns, J. (1975) *Nature (London)* **255,** 197–200.
5. Campbell, F., Williams, G. T., Appleton, M. A. C., Dixon, M. F., Harris, M. & Williams, E. D. (1996) *Gut* **39,** 569–573.
6. Ahuja, N., Li, Q., Mohan, A. L., Baylin, S. B. & Issa, J. P. (1998) *Cancer Res.* **58,** 5489–5494.
7. Toyota, M., Ahuja, N., Ohe-Toyota, M., Herman, J. G., Baylin, S. B. & Issa, J. P. (1999) *Proc. Natl. Acad. Sci. USA* **96,** 8681–8686.
8. Pfeifer, G. P., Steigerwald, S. D., Hansen, R. S., Gartler, S. M. & Riggs, A. D. (1990) *Proc. Natl. Acad. Sci. USA* **87,** 8252–8256.
9. Silva, A. J., Ward, K. & White, R. (1993) *Dev. Biol.* **156,** 391–398.
10. Holliday, R. & Pugh, J. E. (1975) *Science* **187,** 226–232.
11. Bird, A. P. & Wolffe, A. P. (1999) *Cell* **99,** 451–454.
12. Robertson, K. D. & Jones, P. A. (2000) *Carcinogenesis* **21,** 461–467.
13. Nakamura, S., Goto, J., Kitayama, M. & Kino, I. (1994) *Gastroenterology* **106,** 100–107.
14. Clark, S. J., Harrison, J., Paul, C. L. & Frommer, M. (1994) *Nucleic Acids Res.* **22,** 2990–2997.
15. Olek, A., Oswald, J. & Walter, J. (1996) *Nucleic Acids Res.* **24,** 5064–5066.
16. Fisher, L. W., Heegaard, A. M., Vetter, U., Vogel, W., Just, W., Termine, J. D. & Young, M. F. (1991) *J. Biol. Chem.* **266,** 14371–14377.
17. Potten, C. S., Kellett, M., Roberts, S. A., Rew, D. A. & Wilson, G. D. (1992) *Gut* **33,** 71–78.
18. Cannings, C. (1974) *Adv. Appl. Prob.* **6,** 260–290.
19. Williams, E. D., Lowes, A. P., Williams, D. & Williams, G. T. (1992) *Am. J. Pathol.* **141,** 773–776.
20. Booth, C. & Potten, C. S. (2000) *J. Clin. Invest.* **105,** 1493–1499.
21. Zhu, X., Deng, C., Kuick, R., Yung, R., Lamb, B., Neel, J. V., Richardson, B. & Hanash, S. (1999) *Proc. Natl. Acad. Sci. USA* **96,** 8058–8063.
22. Graff, J. R., Gabrielson, E., Fujii, H., Baylin, S. B. & Herman, J. G. (2000) *J. Biol. Chem.* **275,** 2727–2732.
23. Sakurazawa, N., Tanaka, N., Onda, M. & Esumi, H. (2000) *Cancer Res.* **60,** 3165–3169.
24. Shmookler Reis, R. J. & Goldstein, S. (1982) *Proc. Natl. Acad. Sci. USA* **79,** 3949–3953.
25. Loeb, L. A. (1991) *Cancer Res.* **51,** 3075–3079.
26. Cross, S. H. & Bird, A. P. (1995) *Curr. Opin. Genet. Dev.* **5,** 309–314.
27. Xie, T. & Spradling, A. C. (2000) *Science* **290,** 328–330.
28. Tran, J., Brenner, T. J. & DiNardo, S. (2000) *Nature (London)* **407,** 754–757.
29. Kiger, A. A., White-Cooper, H. & Fuller, M. T. (2000) *Nature (London)* **407,** 750–754.
30. Nowell, P. C. (1976) *Science* **194,** 23–28.
31. Martin, G. M., Ogburn, C. E., Colgin, L. M., Gown, A. M., Edland, S. D. & Monnat, R. J., Jr. (1996) *Hum. Mol. Genet.* **5,** 215–221.
32. Laird, P. W., Jackson-Grusby, L., Fazeli, A., Dickinson, S. L., Jung, W. E., Li, E., Weinberg, R. A. & Jaenisch, R. (1995) *Cell* **81,** 197–205.
33. Shoemaker, A. R., Moser, A. R. & Dove, W. F. (1995) *Cancer Res.* **55,** 4479–4485.
34. Tsao, J. L., Yatabe, Y., Salovaara, R., Jarvinen, H. J., Mecklin, J. P., Aaltonen, L. A., Tavaré, S. & Shibata, D. (2000) *Proc. Natl. Acad. Sci. USA* **97,** 1236–1241.